Heliyon 10 (2024) e24782

Contents lists available at ScienceDirect

Heliyon

journal homepage: www.cell.com/heliyon

Research article

Mechanism of action of vinegared Cornu Cervi Degelatinatum in suppressing spleen kidney yang deficient ulcerative colitis through NCK2-JNK pathway

Tianshi Li [a], Mengqi Shi [a,1], Yan Zhao [a,b,c,*], Zhongmei He [a,b,c], Ying Zong [a,b,c], Weijia Chen [a,b,c], Rui Du [a,b,c,**]

[a] College of Chinese Medicinal Materials, Jilin Agricultural University, Changchun, 130118, China
[b] Jilin Provincial Engineering Research Center for Efficient Breeding and Product Development of Sika Deer, Changchun, 130118, China
[c] Key Laboratory of Animal Production and Product Quality and Security, Ministry of Education, Ministry of National Education, Changchun, 130118, China

ARTICLE INFO

Keywords:
Cornu Cervi Degelatinatum
Spleen kidney yang deficiency
Ulcerative colitis
Intestinal flora
NCK2/PAK4/JNK signal pathway

ABSTRACT

Background: As a traditional Chinese herbal medicine, Cornu Cervi Degelatinatum (CCD) has the effect of warming the kidney to support yang, astringing, and stopping bleeding, and is used for spleen kidney yang deficient (SKYD). This experiment was to investigate the therapeutic effects of different processes of CCD on SKYD type ulcerative colitis (UC) rats and to explore its impact on the intestinal flora of rats. Methods: ELISA was used to study the anti-inflammatory activity of Cornu Cervi Degelatinatum processed with water (WCCD) and Cornu Cervi Degelatinatum processed with vinegar (VCCD). 16SrRNA and transcriptome sequencing were used to detect the composition of rat intestinal flora and gene expression; RT-PCR and Western blot were used to verify the role of WCCD and VCCD in treating UC. Results: WCCD and VCCD have therapeutic effects on UC, could reduce tissue damage. VCCD performed better in improving Bacteroidetes/Firmicutes ratios and species evenness and abundance; performed better in increasing the quantity of lactobacillus. VCCD simultaneously inhibit the intestinal inflammatory response through NCK2, PAK4, and JNK signaling pathways. Conclusions: WCCD and VCCD play a

Abbreviations: TCM, traditional Chinese medicine; CCD, Cornu Cervi Degelatinatum; SKYD, spleen kidney yang deficient; UC, ulcerative colitis; WCCD, Cornu Cervi Degelatinatum processed with water; VCCD, Cornu Cervi Degelatinatum processed with vinegar; TNBS, 2,4,6-trinitrobenzene sulfonic acid; SASP, Sulfasalazine; DAI, Disease activity index; CMDI, Colonic mucosal damage index; ELISA, enzyme-linked immunosorbent assay; H&E, hematoxylin-eosin; TNF-α, Tumour Necrosis Factor alpha; IL-6, Interleukin-6; IL-4, Interleukin-4; IL-10, Interleukin-10; IL-1β, Interleukin-1β; PcoA, Principal co-ordinates analysis; OUT, Operational Taxonomic Units; B/F, Bacteroidetes/Firmicutes; SCFAs, short-chain fatty acids; LDA, Linear Discriminant Analysis; GO, gene ontology; BP, biological process; CC, cellular component; MF, molecular function; KEGG, kyoto encyclopedia of genes and genomes; DEGs, differentially expressed genes; RT-qPCR, Real Time Quantitative PCR; ANOVA, analysis of variance; RT-PCR, Reverse Transcription-Polymerase Chain Reaction; NCK2, Cytoplasmic protein NCK2; PAK4, Serine/threonine-protein kinase PAK4; JNK, Stress-activated protein kinase JNK; p-JNK, Phospho-Stress-activated protein kinase JNK.

* Corresponding author. College of Chinese Medicinal Materials, Jilin Agricultural University, Xincheng Street 2888, Changchun, 130118, Jilin China.

** Corresponding author. College of Chinese Medicinal Materials, Jilin Agricultural University, Xincheng Street 2888, Changchun, 130118, Jilin, China.

E-mail addresses: 20210995@mails.jlau.edu.cn (T. Li), 20210978@mails.jlau.edu.cn (M. Shi), zhaoyan@jlau.edu.cn (Y. Zhao), heather78@jlau.edu.cn (Z. He), zongying@jlau.edu.cn (Y. Zong), weijiac@jlau.edu.cn (W. Chen), durui@jlau.edu.cn (R. Du).

[1] Co-first author.

https://doi.org/10.1016/j.heliyon.2024.e24782
Received 22 November 2023; Received in revised form 12 January 2024; Accepted 15 January 2024
Available online 20 January 2024

therapeutic role in UC by regulating the proportion of different flora in the intestinal flora. VCCD regulates the intestinal flora and inflammatory response by interfering with the NCK2, PAK4 and JNK signaling pathways.

1. Introduction

Ulcerative colitis (UC) [1] is a chronic, non-specific inflammatory disease of the rectum and colon, which belongs to inflammatory bowel disease. The lesion is mainly located in the mucosa and submucosa of the large intestine, and its clinical manifestations were abdominal pain, diarrhea, mucus, pus, and bloody stool because of its unclear etiology, long disease course, easy recurrence, and easy carcinogenesis. The incidence of UC has been increasing annually in recent decades, rising from 0.1 to 2.0 per 100,000 to 3.1 per 100, 000 in Asian countries since the 1970s [2]. An epidemiologic survey of UC carcinogenesis showed that colorectal carcinogenesis occurred in 29 of 3561 UC patients, with an overall cancer rate of 0.81 % [3]. Therefore, UC is classified by the WHO as one of the international intractable diseases. UC is prolonged and difficult to cure, and has become a common digestive disease that endangers people's health.

The etiology of UC is complex and the pathogenesis is not fully understood. The main causative factors currently considered include dietary environment, mental and psychological, immune function, genetics, lifestyle and other factors [4]. Ulcerative colitis belongs to the categories of "congestion", "diarrhea" and "resting diarrhea" in Chinese medicine. Spleen deficiency is the root cause of the disease, and prolonged diarrhea injures the kidneys, and spleen yang and kidney yang are unable to warm and nourish each other, which ultimately leads to spleen and kidney yang deficiency [5]. The spleen and kidneys can not be warmed up by each other, which will eventually lead to spleen and kidney yang deficiency. Some studies have found that spleen and kidney yang deficiency has the highest frequency in the distribution of Chinese medicine symptoms of UC, which shows that spleen and kidney yang deficiency is an important pathogenetic mechanism of UC, and therefore spleen and kidney yang deficiency is a common and prevalent pattern of UC. Although the current clinical use of aminosalicylic acid, glucocorticoids, probiotics and other drugs have a certain degree of efficacy, but still can not remove the root cause of the disease, once the drug is discontinued, the risk of relapse. Long-term use of these drugs may also lead to complications such as drug resistance, allergic reactions, liver toxicity and kidney damage [6]. In recent years, research has found that Chinese medicine and the combination of traditional Chinese medicine (TCM) and Western medicine can not only improve the local ulcer symptoms of patients, and Chinese medicine side effects are small, not easy to recur, long-term efficacy, in the clinical treatment of UC to achieve more satisfactory results. Therefore, it is more worthwhile for us to explore and promote the characteristic advantages of TCM in treating UC by combining the traditional theoretical ideas of TCM with the cutting-edge research of modern medicine.

As a traditional animal medicine, cornu cervi degelatinatum has been used in China for more than 2000 years, The *Chinese Pharmacopoeia (2020)* records that cornu cervi degelatinatum has the efficacy of warming the kidney and assisting the yang, astringing and stopping bleeding, and is commonly used in the treatment of spleen and kidney yang deficiency, sores and ulcers that do not astringent and other conditions [7]. Chinese medicine concoction is an important link in the system of Chinese medicine and an intangible requirement for the evidential, discriminative and complex nature of Chinese medicine. Vinegar processing has a wide range of applications and a large number of applications. According to statistics, there are 251 varieties of TCM vinegar in the past dynasties, among which there are 17 kinds of vinegar processing methods. It can be seen that vinegar processing is one of the essential methods in the processing of TCM. Modern pharmacological research has found that vinegar processing can improve the efficacy of TCM, reduce the toxicity of TCM and improve the solubility of active ingredients of TCM [8]. Vinegar-processed deer cornu cervi degelatinatum was firstly seen in *Lei Gong Pao Zhi Lun (Master Lei's Discourse on Medicinal Processing)* [9]. Still, until now, there is no relevant study on the differences between vinegar-processed cornu cervi degelatinatum and water-processed cornu cervi degelatinatum in terms of chemical composition and pharmacological effects.

In this study, the differences in the chemical composition of the two cornu cervi degelatinatums were analyzed by analyzing the changes in the content of amino acids and minerals. Using 16S rRNA and transcriptomics methods, we analyzed the differences in pharmacological effects of the two cornu cervi degelatinatums in the treatment of spleen and kidney yang deficiency type ulcerative colitis and their related mechanisms.

2. Materials and methods

2.1. Reagents and chemicals

Amino acid reference substance was purchased from Sigma (USA). Multi-element mixed standard solution and sodium carboxymethyl cellulose were purchased from Shanghai McLean Biochemical Technology Co., Ltd. (Shanghai, China). Nitric acid, perchloric acid and hydrochloric acid were purchased from Shanghai Aladdin Biochemical Technology Co., Ltd. (Shanghai, China). Antler plates were purchased from Jilin lushengyuan animal and plant Sightseeing Park Co., Ltd. (Changchun, China). Senna leaves were purchased from Jilin Changchun fubaicao pharmacy. Hydrocortisone was purchased from Sinopharm Rongsheng Pharmaceutical Co., Ltd. (Henan, China). Trinitrobenzene sulfonic acid 5 % aqueous solution (2,4,6-TNBS). Avodin was purchased from Sigma. Sulfasalazine (SASP) was purchased from Shanghai XinyiTianping Pharmaceutical. Normal saline was purchased from Sichuan Kelun Pharmaceutical Co., Ltd. Ethanol was purchased from gyp reagent. Rat TNF-α, IL-1β, IL-6, IL-4, IL-10 enzyme-linked immunosorbent assay kit

was purchased from Jiangsu Boyan Biotechnology Co. Ltd (Jiangsu, China). TRIzol reagent and RT-qPCR kit were purchased from Thermo Scientific (Jiangsu, China). Antibody NCK2 and PAK4 were purchased from Wuhan Three Eagles Biotechnology Co Ltd (Wuhan, China). Antibody JNK, p-JNK and β-actin were purchased from Wan Class Biotechnology Co. Ltd (Shenyang, China). Goat Anti-Rabbit IgG/HRP was purchased from Solarbio (Beijing, China). All chemicals used were of analytical grade.

2.2. Sample preparation

2.2.1. Preparation of WCCD

According to the processing method of cornu cervi degelatinatum in *Chinese Pharmacopoeia (2020)*, add 800 mL of water to every 100 g of red deer (*Cervus canadensis*) antler powder, heat it at 120 °C for 2 h, filter it, add 800 mL of water to the filter residue, heat it at 100 °C for 1 h, Collect the filter residue and dry it [7].

2.2.2. Preparation of VCCD

Based on the processing method of vinegar-processed cornu cervi degelatinatum in *Lei Gong Pao Zhi Lun*, with modifications, add 800 mL of vinegar to every 100 g of red deer (*Cervus canadensis*) antler powder, heat it at 120 °C for 2 h, filter it, add 800 mL of vinegar to the filter residue, heat it at 100 °C for 1 h, Collect the filter residue and dry it [9].

2.3. Chemical composition difference between wccd and vccd

2.3.1. Determination of amino acid content

Take 16 kinds of amino acid reference materials, weigh them accurately, add 20 mol/L hydrochloric acid solution to dissolve, and dilute them to a concentration of 1 μmol/mL of mixed reference stock solution. Accurately measure 2 mL into a 100 mL volumetric flask, add 20 mol/L hydrochloric acid solution to the scale, shake well, and use it as the reference solution.

The prepared WCCD and VCCD were crushed, sieved through 60 mesh sieve respectively, weighed 30 mg of powder with precision, added 5 mL of 6 mol/L hydrochloric acid solution, filled with high purity nitrogen, and quickly sealed in a blowtorch, and then placed in the 110 °C constant temperature drying oven, hydrolyzed for 24 h, and fixed to 25 mL. Pipetted 0.5 mL of the filtrate into a centrifugal tube, remove the solvent with a vacuum centrifugal concentrator, and evaporate it 1–2 times at 60 °C. Add 1 mL of sample dilution solution to redissolve, filtered with 0.22 μm aqueous microporous filter membrane, as the test solution.

The reference solution and the test solution were respectively injected into the amino acid analyzer with the same volume, and the concentration of amino acids in the sample determination solution was calculated by the external standard method through the peak area [10].

2.3.2. Determination of mineral element content

WCCD and VCCD samples were mixed evenly at high speed, respectively. Accurately weigh 0.5 g of the sample in the microwave digestion jar, add 5 mL of nitric acid, and place it in the microwave digestion instrument for digestion [11]. After digestion, place the digestion tank on the acid-driving rack and heat it at 150 °C to drive the acid to near dryness. After cooling, transfer the digestion solution to a 25 mL volumetric flask for constant volume. The standard solution and sample solution were injected into the inductively coupled plasma mass spectrometer to measure the signal response values of the elements to be measured and the internal standard elements, and the concentration of the elements to be measured in the digestion solution was obtained according to the standard curve.

2.4. Experimental animals

72 seven week old male Sprague-Dawley (SD) rats (200–220 g) were purchased from Changchun Yisi Laboratory Animal Technology Co., LTD (Changchun, China), animal license No. SYXK (Ji) 2018-0023. The experimental animals were placed in an environment with a room temperature of 20–25 °C, humidity of 60 ± 5 %, and light dark cycle of 12 h. They were given a standard diet and distilled water to eat freely and had a week of adaptation. The relevant materials of animal experiments involved in this study were reviewed by the experimental animal welfare and ethics committee of Jilin Agricultural University (Permit number: 20211011003). The project is considered to meet the ethical requirements of experimental animals.

2.5. Establishment of spleen kidney yang deficiency (SKYD) type rat with ulcerative colitis (UC)

After one week of adaptive feeding, 64 rats were randomly selected for modeling, the SKYD was reproduced by senna and hydrocortisone. 15 % Senna solution was gavaged at 2 mL/100 g, and hydrocortisone 10 mg/kg was injected intraperitoneally for 21 days. The control group was given normal saline. Trinitrobenzene sulfonic acid (TNBS)/ethanol enema was used to replicate the UC model [12]. After fasting for 24 h, but with water, anesthesia was performed with 1.25 % tribromoethano 10 mL/kg intraperitoneally. After successful anesthesia, take a silicone tube with a length of about 10 cm to draw a mixed solution of 100 mg kg^{-1} TNBS and 55 % ethanol in the same volume ratio; slowly insert the silicone tube coated with paraffin oil into the anus for about 8 cm, and then slowly push the modeling solution into the colon with a syringe. After injection of the modeling solution, the rats' tail was lifted and inverted for 1–2 min to ensure that the modeling solution could be diffusely distributed in the rat intestine. The control group was enema with normal saline. After modeling, the rats were put into the cage for routine feeding after they were awake.

2.6. Experimental design

After successful modeling, the rats were randomly divided into 8 groups: model group (TNBS), positive control group (SASP) , 3.37 g/kg of WCCD-treated group [WCCD(L)], 6.75 g/kg of WCCD-treated group [WCCD(M)], 13.5 g/kg of WCCD-treated group [WCCD (H)], 3.37 g/kg of VCCD-treated group [VCCD(L)], 6.75 g/kg of VCCD-treated group [VCCD(M)] and 13.5 g/kg of VCCD-treated group [VCCD(H)]. The control and TNBS group was given equal volume of normal saline by gavage at the same time. SASP group, WCCD(L) group, WCCD(M) group, WCCD(H) group, VCCD(L) group, VCCD(M) group, and VCCD(H) group were orally administered sulfasalazine (i.g, 0.35 g/kg/d), WCCD (i.g, 3.37 g/kg/d), WCCD (i.g, 6.75 g/kg/d), WCCD (i.g, 13.5 g/kg/d), VCCD (i.g, 3.37 g/kg/d), VCCD (i.g, 6.75 g/kg/d), and VCCD (i.g, 13.5 g/kg/d) for 21 days. On the last day, all rats were anesthetized with tribromoethano, and their blood and colon tissues were collected [12].

2.7. Disease activity index (DAI) scoring

Observations on body weight, mental status, coat luster, dietary status, fecal texture and fecal occult blood of rats. Fecal occult blood test: A small amount of feces was smeared on the center of a slide, and 3 drops of 10 g/L cresyl sulfate and 3 % hydrogen peroxide solution were added to the feces, and the results were observed after mixing. Disease activity DAI score [5] was performed based on the general condition of the rats, and the DAI score was the average of the weight loss score, the fecal character score and the fecal occult blood score. The specific scoring criteria are shown in Table 1.

2.8. Colonic mucosal damage index (CMDI) scoring

After 21 days of treatment, fasting for 24 h, but water. After dissecting the rats, the colon tissue of each group of rats was obtained, and the morphology of the affected colon and the damage to the colon mucosa were observed with the naked eye [5]. The CMDI was scored according to the following Table 2.

2.9. Monitoring of dietary (water) content

The dietary (water) content of rats in each group was monitored after treatment and recorded in detail in each group.

2.10. Histological evaluation by hematoxylin and eosin

After rats were sacrificed, the colon was quickly removed, rinsed with ice-cold phosphate buffer solution (PBS), and the excess PBS was removed. The tissue samples were immediately fixed in 10 % neutral formalin solution and embedded in paraffin. 4 μm serial sections were stained with hematoxylin-eosin (HE), and the pathological changes of colon tissues were observed under the microscope. HE sections were evaluated based on the number of inflammatory cells and tissue damage; the more inflammatory cells, the more severe the tissue damage.

2.11. Enzyme linked immunosorbent assay(ELISA)

After rats were sacrificed, the serum was collected by centrifugal tube. After 30 min of agglutination, the blood sample was centrifuged at 2000 rmp for 10 min. Detect the serum samples immediately after taking them, or subpackaged and stored at −80 °C to avoid repeated freezing and thawing. Strictly following the operation method of the kit, The concentrations of TNF-α, IL-6, IL-4, IL-10, and IL-1β were detected by Elisa [13].

2.12. 16SrRNA sequencing analysis of colon microorganism

2.12.1. Genomic DNA extraction and PCR amplification

CTAB or SDS extracted the genomic DNA of the sample, and then the purity and concentration of the extracted DNA were detected by agarose gel electrophoresis [14]. Subsequently, a proper amount of DNA was taken in a centrifuge tube and diluted to 1 ng/μl with sterile water. Diluted genomic DNA was used as a template and specific primers with barcode and Phusion from New England Biolabs'

Table 1
Disease activity index (DAI).

Body weight loss (a)	Stool traits(b)	Stool occult blood(c)	Score
0	Normal	Normal	0
1%–5%	Among	Among	1
6%–10 %	Loose stools	Occult blood positive	2
11%–15 %	Among	Among	3
>15 %	Watery diarrhea	Dominant hemorrhage	4
DAI= (a + b + c)/3			

Table 2
Colonic mucosal damage index (CMDI).

Score	Colon tissue characteristics
0	No damage
1	Local congestion, edema, no erosion or ulcer
2	Mucosal congestion and edema, mild erosion, no ulcer
3	Mucosal congestion and edema, moderate erosion, single ulcer
4	Mucosal congestion and edema, high erosion, multiple ulcers
5	Mucosal congestion and edema, severe erosion, with >1 cm ulcers

Phusion® High-Fidelity PCR Master Mix with GC Buffer and high-efficiency high-fidelity enzymes were used for PCR to ensure amplification efficiency and accuracy.

2.12.2. Mixing and purification of PCR products

PCR products were detected by agarose gel electrophoresis at a concentration of 2 %, and equal amounts of samples were mixed according to the concentration of PCR products. After thorough mixing, agarose gel electrophoresis was used for detection again, and the target band was recovered using the gel recovery kit provided by Qiagen.

2.12.3. Library construction and computer sequencing

The library was constructed using NEBNext® Ultra™ II DNA Library Prep Kit, and Qubit and Q-PCR quantified the built library. After the library was qualified, novaseq6000 was used for computer sequencing.

2.12.4. Sequencing data processing

Microbial-related data each sample data was split from the offline data according to the barcode sequence and PCR amplification primer sequence. After the barcode and primer sequences were truncated, the reads of the samples were spliced using Flash software to obtain Raw Tags. Then, fastq software was used to perform quality control on the Raw Tags, and high-quality clean tags were obtained. Research software was used to compare Clean Tags with the database to detect chimeras and remove them to get the final effective data, namely Effective Tags.

2.13. Colon tissue transcriptome assay

2.13.1. Sample total RNA extraction and quality control

After dissection, the colon of rats was taken and washed repeatedly with PBS until it was clean. Total RNA was extracted by the Trizol method, and colon samples of 3 rats in each model group and the vinegar-processed cornu cervi degelatinatum group were extracted. Nanodrop2000 measures the concentration and purity and records the concentration of each sample and the values of OD260/280 and OD260/230. The integrity of RNA was detected by agarose gel electrophoresis. Finally, the image was observed by the gel imaging system. Agilent210 determines the RNA integrity coefficient, and the sequencing library can be constructed after ensuring its high quality [15].

2.13.2. mRNA library construction and sequencing

Sequencing libraries were mainly constructed using Hieff NGS™ MaxUp Dual-mode mRNA Library Prep Kit for Illumina®. Subsequently, mRNA isolation and fragmentation, double-stranded cDNA synthesis, and linker ligation were carried out, and the final library was obtained by library amplification. Using a Qubit DNA detection kit to accurately quantify the recovered DNA to facilitate sequencing after mixing in equal amounts according to the ratio of 1:1. Clonal clusters were generated by bridge PCR amplification on Illumina's C BOT system and sequencing while synthesizing.

2.13.3. Sequencing data statistics and quality control

The Illumina platform sequencing process captured the fluorescent signal carried by each base, converted it into a text signal by base recognition, and stored it in fastq format as raw data (raw reads). Use fastx_toolkit to evaluate the quality of raw reads of samples. Then, use Sickle and Seq Prep to control the quality of raw reads and get high-quality control data (clean reads).

2.13.4. RNA-Seq data analysis

Hisat2 was applied to compare the fastq file stored with clean reads with the reference genome index, determine the gene sequence corresponding to each read, and output the mapped reads for subsequent analysis (mapped reads). Using Rseqc to count the distribution of mapped reads. The number of Reads for each gene obtained by sequence alignment was counted using RSEM and converted to TPM.

2.13.5. Analysis of differences in expression between groups

After counting the gene expression of each sample, R language was applied to load the expression matrix and set the grouping. Deseq2 was used for analysis, and Benjamini Hochberg corrected the p-value for multiple testing, i.e., FDR. When FDR <0.05, the

experimental group/control group difference multiple (FC) ≥ 1.5 or FC ≤ 0.5, that is, $|\log2FC| \geq 1$. It was considered that the gene expression was significantly different between groups, and DEGs with significant differences between groups could be statistically analyzed.

2.13.6. Cluster analysis of samples and differential genes

Based on the expression matrix of DEGs generated by difference analysis, the samples and DEGs were clustered by R language, and the clustering heat map was derived. The Euclidean algorithm used complete linkage to measure the distance between two gene combination clusters. A single link measured the distance between two sample combination clusters. Accordingly, the gene expression in the sample can be analyzed.

2.13.7. Go and KEGG analysis

After loading the GO library information file, the Python package goatools was applied to perform GO enrichment analysis on DEGs. Fisher's exact test was used to test the significance, and the Bonferroni method was used to correct the p-value. When p-adjust < 0.05, it was considered that DEGs were significantly enriched in this GO function so that the main GO functions of DEGs could be finally obtained. The Kobas website was used for KEGG enrichment analysis. The calculation principle, inspection method, and p-value correction method were similar to GO enrichment analysis and finally found the KEGG pathways that were significantly enriched in DEGs.

2.14. Real-time quantitative polymerase chain reaction (RT-qPCR)

Take an appropriate amount of colon specimen and grind it thoroughly. Total RNA was extracted with a TRIzol reagent, and the RNA concentration was determined. The total RNA was reverse transcribed into cDNA using the RT-qPCR Kit (transgenic biotech, Beijing) for PCR reaction determination. The PCR conditions were pre-denaturation at 94 °C for 5 min and denaturing at 94 °C for 30 s. β-actin was selected as the experimental reference gene, RT-qPCR was used to detect the relative expression of NCK2, PAK4, and JNK and p-JNK. PCR primers for target genes were designed and synthesized by Sangon Biotech (Shanghai) Co., Ltd., as shown in Table 3.

2.15. Western blot

Colon tissues were homogenized in ice-cold Ripa lysate (strong) (pH = 7.4). The buffer was composed of Tris (50 mM), NaCl (150 mM), Triton X-100 (1 %), sodium deoxycholate (1 %), SDS (0.1 %), sodium orthovanadate, sodium fluoride, EDTA, leupeptin and other inhibitors. The concentration of protein extract was detected by a BCA protein concentration assay kit (Thermo Fisher Scientific), and equal amounts of protein were separated by 10 % polyacrylamide gel electrophoresis (10 μg). Then, the protein was transferred to the PVDF membrane, and the PVDF membrane was blocked with skimmed milk at room temperature for 2 h. PVDF membranes were washed in tris-buffered saline containing 0.05 % Tween 20 with primary antibodies NCK2 (1:1000), PAK4 (1:2000), JNK (1:1000), and p-JNK (1:1000) overnight at 4 °C. After incubation with a primary antibody, the membrane was incubated with a secondary antibody (1:5000). The protein bands were visualized using an ECL reagent (Sigma). The gray value of protein bands in the internal reference sample was determined, and the gray value of protein bands was taken as the relative level of the sample.

2.16. Statistical analysis

Statistical analysis was performed by using one-way analysis of variance (ANOVA) with GraphPad Prism version 9.0 (GraphPad Software, San Diego). The quantitative data were shown as the mean ± SD. Data comparisons were conducted following two-tailed Student's t-test. P-value < 0.05 was considered statistically significant.

Table 3
Primer sequence of genes.

Gene name	Sequence (5′–3′)
NCK2	Forward: CTATGTGGTTGTCCTCAGTGATGGG
	Reverse: CGTGCTCGCTGGTGAAGATGG
PAK4	Forward: GATGATTCGGGACAACCTGCCA
	Reverse: AGGAATGGGTGCTTCAGCAGCT
JNK	Forward: AACAGCTCGGAACACCTTGT
	Reverse: AACAGCTCGGAACACCTTGT
p-JNK	Forward: AGTGACAGTAAAAGCGATGGTC
	Reverse: AGCACAAACAATTCCTTGGGC
β-actin	Forward: AGCCTTCCTTCCTGGGCATGGA
	Reverse: GGACAGCACCGTGTTGGCGTAGA

3. Results

3.1. WCCD and VCCD amino acid content

The types and amounts of amino acids contained in WCCD and VCCD are shown in Table 4. The total amount of amino acids in VCCD was 22.6 g/100 g, and that in WCCD was 17.3 g/100 g. The complete amino acid content of VCCD was significantly higher than that of WCCD. Gly, Glu, and Asp account for 42.25%–42.65 % of the total amino acids. Asp and Glu are both acidic amino acids that play an essential role in maintaining normal intestinal function, digestion, absorption and metabolism of nutrients, secretion of hormones, antioxidant capacity, and immunity. Gly can accelerate the decomposition and transformation of glycogen, fat, protein, and other nutrients in the human digestive system, provide energy sources and essential nutrients for the human body, promote metabolism, and improve the immune system's ability.

3.2. WCCD and VCCD mineral element content

CCD was rich in mineral elements, and the content of mineral elements in CCD processed by different methods is different. The differences between P, Mg, Fe, Zn, Al, S, and Cl were more pronounced. The types and contents of mineral elements in WCCD and VCCD are shown in Table 5. It can be seen that the mineral content in VCCD is significantly higher than that in WCCD.

Chemical composition was the internal basis for determining the pharmacological effect of drugs, and the different content and distribution of chemical composition promote different pharmacological effects of drugs. According to the difference in chemical composition between WCCD and VCCD, it can be found that VCCD contains more components, so that VCCD may have more substantial pharmacological effects.

3.3. WCCD and VCCD can alleviate TNBS induced diarrhea

The rats in the control group had a good mental state, glossy fur color, and no obvious changes in diet and feces. On the 3rd day, the rats in the model group started to have unformed feces, but there was no significant change in body weight and mental status. On the 7th day of the model group, the rats were depressed, with dull hair color, reduced diet, slow reaction, and body temperature began to drop. On the 21st day of the model group, the rats showed dilute watery stools, depressed spirit, lusterless or even shedding fur, bunching and gathering, obvious sagging of the scrotum, more frequent defecation, and slow weight gain. Fig. 1A represents the changes in body weight of rats in each group in the experiment; the body weight of the model group was significantly reduced and increased slowly compared with the control group; the growth trend was restored in each administered group compared with the model group. Compared with the WCCD(M) group, the weight growth of the VCCD(M) group was closer to that of the control group. After drug administration, the amount of diet (water) was significantly reduced in all rats in TNBS group compared to control group ($P < 0.05$). The diet (water) of rats in all drug groups was significantly increased ($P < 0.05$) compared to the model group. The increase in diet (water) was more significant ($P < 0.05$) in the VCCD(M) group compared to the WCCD(M) group (Fig. 1E and F).

3.4. Comparison of DAI scores

DAI scores were firstly performed for each group of rats, and there was no significant change in the DAI scores of control rats. On the 2nd day after TNBS was pushed into the colon, rats in each group showed watery stools, perianal contamination, feces with mucus or even blood, naked eyes, withered hair, curled up and lethargic, and weight loss and emaciation. By the fourth week of membrane creation, the DAI score was the highest. Compared with the control group, the DAI scores of rats in all groups were significantly higher, and the difference was statistically significant ($P < 0.05$); in the first week after the gavage treatment, the rats in the WCCD and VCCD groups showed gradual improvement in their spirit, increased food intake, increased body weight, and improved fecal quality, and the DAI scores were significantly reduced, and the difference was statistically significant ($P < 0.05$); from the sixth to the seventh week, the DAI scores slowly decreased (Fig. 1B). Meanwhile, the DAI scores of rats in the VCCD(M) group at the end of drug administration were significantly lower than those of the other groups ($P < 0.05$; Fig. 1C).

Table 4
Amino acid content in samples (g/100 g).

Type	WCCD	VCCD	Type	WCCD	VCCD
Ile	0.35	0.38	Ser	0.67	0.83
Leu	0.87	0.99	Glu	2.41	2.72
Tyr	0.22	0.25	Pro	2.05	2.91
Ala	1.75	2.32	Gly	3.44	5.21
Val	0.64	0.72	Phe	0.52	0.62
Met	0.14	0.12	His	0.29	0.3
Asp	1.46	1.71	Lys	0.74	0.99
Thr	0.46	0.55	Arg	1.32	1.99

Table 5
Content of mineral elements in samples (g/100 g).

Type	WCCD	VCCD	Type	WCCD	VCCD
Na	0.0037	0.0057	K	0.0372	0.6978
Mg	0.2549	0.2411	Ca	51.8288	55.2457
Al	0.0026	0.0037	Fe	0.3059	0.3865
P	1.5856	1.3920	Zn	0.0024	0.0031
S	0.3617	0.4327	As	0.0032	0.0040
Cl	9.4544	11.6282	Sr	0.0125	0.0137

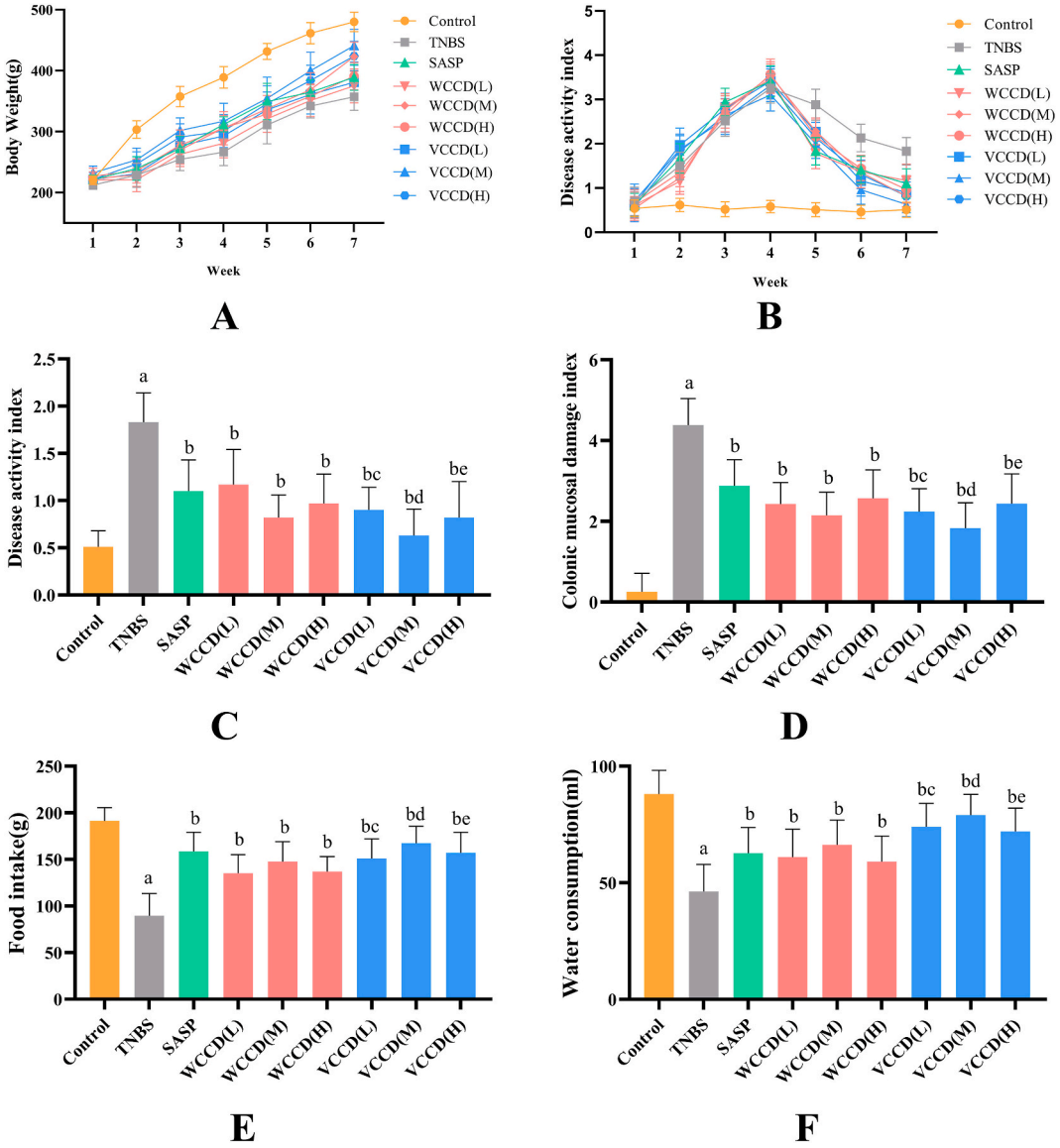

Fig. 1. WCCD and VCCD improved TNBS induced UC rat. (A) Body weight. (B and C) The DAI socre. (D) The CMDI score. (E) Food intake. (F) Water consumption. Different letters indicated statistically significant differences, compared to the control group, $^{a}P < 0.05$; compared to the model group, $^{b}P < 0.05$; compared to the WCCD(L) group, $^{c}P < 0.05$; compared to the WCCD(M) group, $^{d}P < 0.05$; compared to the WCCD(H) group, $^{e}P < 0.05$. Data are means ± SD (n = 8).

3.5. Comparison of CMDI scores

CMDI scoring was performed on the colon condition of rats in each group. The colon surface of rats in the control group was smooth and clean, without foreign matter, with normal morphological luster, intact tissues, clear vascular texture, and no tissue adhesion. In the model group, there were feces adhering to the intestinal wall in the colon, the intestinal mucosa was congested and edematous, some colons and surrounding tissues were adherent and not easy to be separated, the vascular texture of the intestinal mucosa was blurred, disorganized, or disappeared, and the surface of the mucosa was diffusely granular, with erythema or hemorrhage. Compared with the control group, the CMDI score was significantly higher in the model group, and the difference was statistically significant ($P < 0.05$) (Fig. 1D). Compared with the model group, after administration of WCCD and VCCD, the degree of colonic mucosal damage in rats improved, and although some colons and surrounding tissues were still adherent, the ulcerated surfaces were significantly reduced, and the CMDI scores were all significantly reduced ($P < 0.05$); among them, the CMDI scores of the colons of rats in the VCCD (M) group were significantly lower than that of the other groups ($P < 0.05$) (Fig. 1D).

3.6. HE staining pathological damage of colon tissue

As shown in Fig. 2, in the control group, the colonic mucosal layers were clear, the crypt structure was clear, the mucosa was intact, the muscularis layer was visible, the glands were neatly arranged, the depressions were tightly aggregated, and the thrush cells were evenly distributed, and no damage was seen. In the model group, the integrity of the colonic tissue was damaged, the glands in the lamina propria were reduced, the crypt structure was deformed, and a large number of inflammatory cells infiltrated directly into the muscularis propria; many fibroblasts and collagen fibers were found in the muscularis propria, forming granulation tissue, with varying degrees of congestion, edema, and ulceration; and the wall of the colonic was obviously thickened (Fig. 2). Compared with the model group, the epithelium of the WCCD and VCCD groups had different degrees of recovery, the crypt structure was partially altered, the lymphocytes and neutrophils were reduced, the myenteric layer was slightly repaired but still fractured, and the degree of tissue damage was significantly lower than that of the model group, although the colon still contained a small number of inflammatory cells

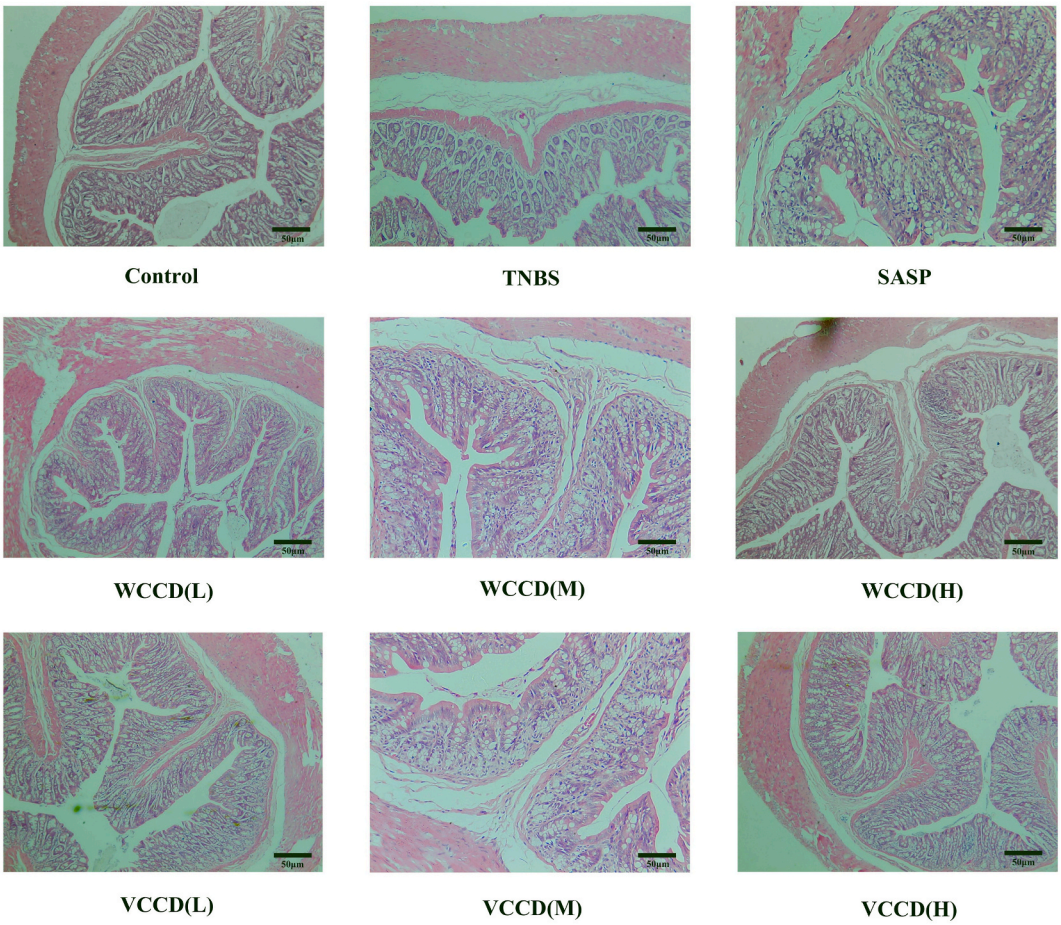

Fig. 2. H&E staining of colon tissue in each group (magnification × 100).

(Fig. 2). Meanwhile, compared with the WCCD group, the colonic structure of the VCCD group was relatively complete and clear, which was already close to the normal tissue structure (Fig. 2).

3.7. WCCD and VCCD alleviate TNBS induced intestinal inflammation

As the degree of colonic inflammation increases, imbalance in the expression of pro-inflammatory and anti-inflammatory factors in serum plays an important role in the development and progression of colonic inflammation. Therefore, we determined the differences in serum inflammatory factors in rats with ulcerative colitis treated with two different CCD processing methods (Fig. 3). As shown in Fig. 3, the levels of pro-inflammatory cytokines IL-6, TNF-α, and IL-1β were significantly higher in rats in the TNBS model group compared with the control group ($P < 0.05$; Fig. 3B–D, E); and the levels of anti-inflammatory factors IL-4 and IL-10 were significantly lower ($P < 0.05$; Fig. 3A–C). Compared with the model group, the levels of pro-inflammatory cytokines IL-6, TNF-α, and IL-1β were significantly lower in rats in the SASP, WCCD, and VCCD groups ($P < 0.05$; Fig. 3B–D, E); and the levels of inflammation-suppressing factors IL-4 and IL-10 were significantly higher ($P < 0.05$; Fig. 3A–C). This indicated that both WCCD and VCCD could improve the changes of serum inflammatory factors in rats caused by TNBS, thus reducing colonic inflammation. Compared with the WCCD group, the serum of rats in the VCCD group had a more significant down-regulation ($P < 0.05$) of IL-6, TNF-α and IL-1β, and a more significant up-regulation ($P < 0.05$) of IL-4 and IL-10, suggesting that the VCCD improved the changes of inflammatory factors in rats with ulcerative colitis better than the WCCD. Meanwhile, the serum IL-4 and IL-10 levels of rats in the VCCD(M) group were significantly higher than those in other administered groups ($P < 0.05$; Fig. 3A–C); and the serum IL-6, TNF-α and IL-1β levels of rats in the VCCD(M) group were significantly higher than those in other administered groups ($P < 0.05$; Fig. 3B–D, E).

3.8. 16S rRNA sequencing analysis

Through the early pharmacological effects of WCCD and VCCD, we found that the therapeutic effects of WCCD and VCCD on ulcerative colitis were superior to those of SASP. Therefore, we performed 16S rRNA sequencing analysis on the feces of rats in the WCCD(M) and VCCD(M) groups, to verify whether the different concoctions of Cornu Cervi Degelatinatum were effective in regulating the intestinal flora.

Our results showed that good habitat diversity was present in all samples (Fig. 4A). In addition, WCCD(M) and VCCD(M) significantly altered the species diversity, especially the β-diversity, in the colon of UC rats (Fig. 4B), which could be found to be more similar between the VCCD(M) and Ctrl groups. The overall assessment of the colonic microbiota of each group using PCoA, with axis 1 (PCoA1) explaining 47.8 % of the variability and axis 2 (PCoA2) explaining 22.34 %, showed that the microbial species were very different between the TNBS and Ctrl groups, and the samples were almost completely segregated. The clustering of microorganisms in the VCCD(M) group versus Ctrl group was more similar than that in the WCCD(M) group was more similar to the clustering of microorganisms in the Ctrl group (Fig. 4C). Fig. 4D shows the distribution of the more abundant genera in the rat colon microorganisms in

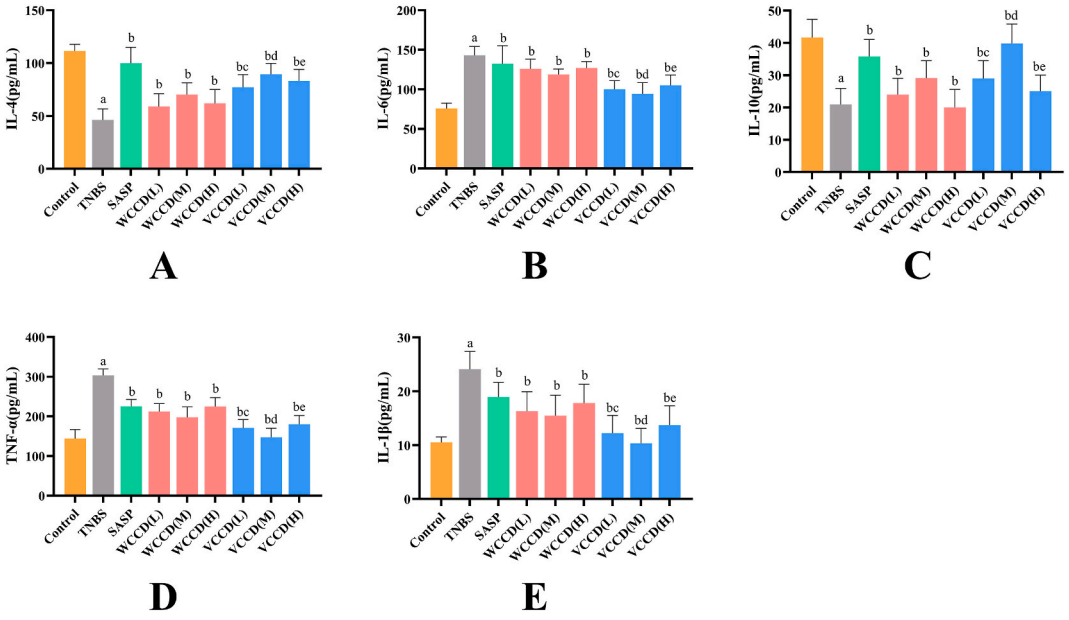

Fig. 3. WCCD and VCCD treatment reduces the inflammatory response. A–E: Expression level of IL-4, IL-6, IL-10, TNF-α, IL-1β in rats. Different letters indicated statistically significant differences, compared to the control group, $^{a}P < 0.05$; compared to the model group, $^{b}P < 0.05$; compared to the WCCD(L) group, $^{c}P < 0.05$; compared to the WCCD(M) group, $^{d}P < 0.05$; compared to the WCCD(H) group, $^{e}P < 0.05$. Data are means ± SD (n = 3).

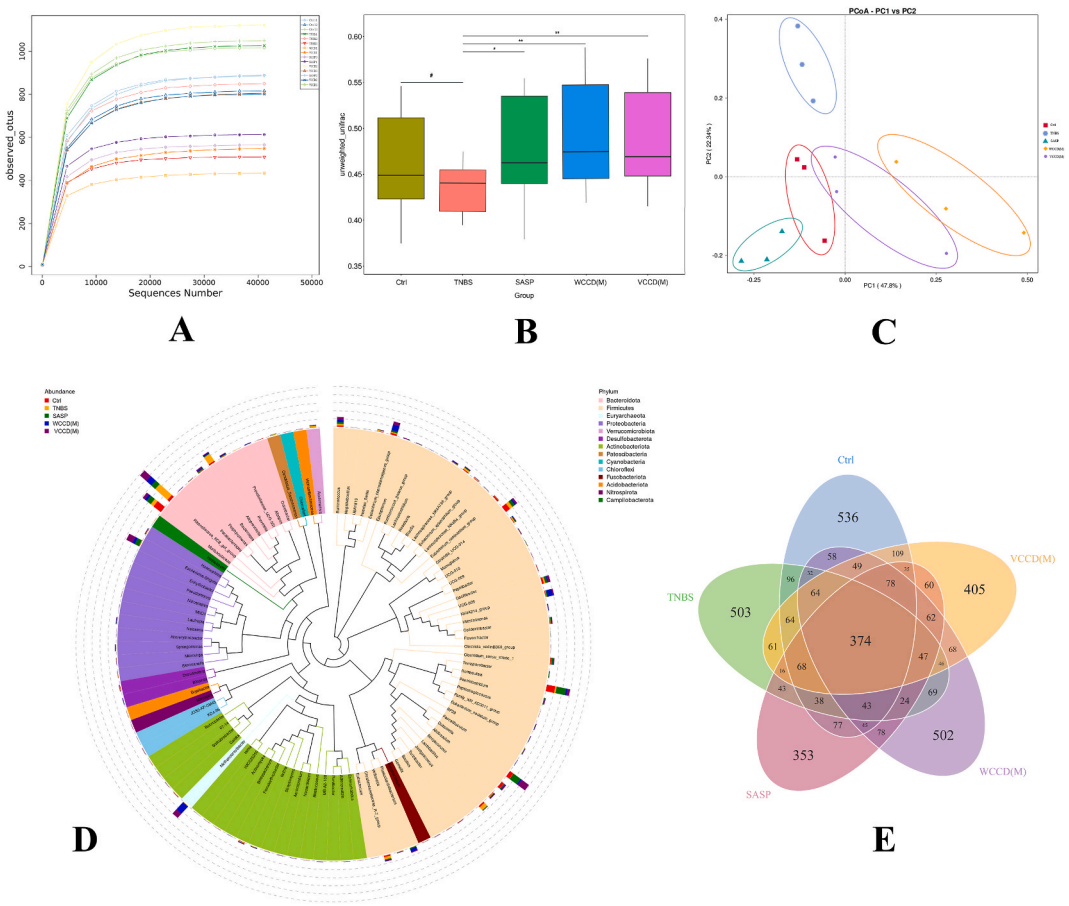

Fig. 4. Treatment with WCCD(M) and VCCD(M) improves intestinal flora in TNBS rats. (A) Observed species. (B) Unweighted unifrac wilcox demonstrated the β-diversity. (C) The principal coordinates analysis (PCoA) demonstrated distinct structural changes in the overall bacterial population. (D) The phylogenetic relationships of top 100 genus level species. (E) Venn diagram of the species. $^{\#}p < 0.05$ vs the ctrl group (decreased); $^{*}p < 0.05$, $^{**}p < 0.01$ vs the TNBS group (elevated). Data are means ± SD (n = 3).

each group, and the more abundant ones in the model group were the harmful bacteria *Helicobacter pylori*, *Shigella*, and *Enterobacter* spp. The number of beneficial bacteria *Lactobacillus* was significantly increased, and the number of *Erysipelothrix Rosenbach* and *Chaetomiaceae* was significantly decreased after the treatment of VCCD(M) (Fig. 4D), whereas the change was insignificant after the treatment of WCCD(M). The Venn flower map based on OTU displayed OTU differences among the different groups (Fig. 4E).

In addition, a significant decrease in various genera was found in the TNBS rat, such as *Lactobacillus*, *Bacteroides*, *Ruminococcus*, and *Intestinimonas*, increasing the probability of diarrhea. The treatment with VCCD(M) resulted in a significant increase in the number of *Lactobacillus*. (Fig. 5A and B). It can also be found that WCCD(M) and VCCD(M) treatments resulted in a significant increase in the content of intestinal microorganisms *Lactobacillus* and *Firmicutes* (Fig. 5A and B), and the increase in the content of *Lactobacillus* and *Firmicutes* was more pronounced in the VCCD(M) group, which suggests that the restoration of the intestinal flora of the rat was more pronounced with VCCD(M). The LDA score represents the impact of different species, with a greater value representing a greater impact of different species. The difference in *Lactobacillus* between the VCCD(M) rat and the other groups was the largest compared to the TNBS group rat (Fig. 5C). Furthermore, the analysis revealed that the abundance of *Firmicutes*, *Bacteroidota*, and *Deferribacteres* varied significantly in the TNBS rat.

The experimental results combined with those above demonstrated that our drug could significantly regulate the intestinal microbiota of TNBS rat, and the content of beneficial bacteria in the VCCD(M) group is more and similar to the microbial structure of the control group, suggesting that VCCD(M) is more favorable to the recovery of the disease.

3.9. Differentially expressed genes

By comparing the early pharmacological effects of WCCD and VCCD, and the effects of WCCD(M) and VCCD(M) on the intestinal flora of rats, we found that the therapeutic efficacy of VCCD on ulcerative colitis was superior to that of WCCD. Therefore, we carried out transcriptomics analysis on the colons of rats from the VCCD(M) group, in order to explore the mechanism of VCCD(M) in the

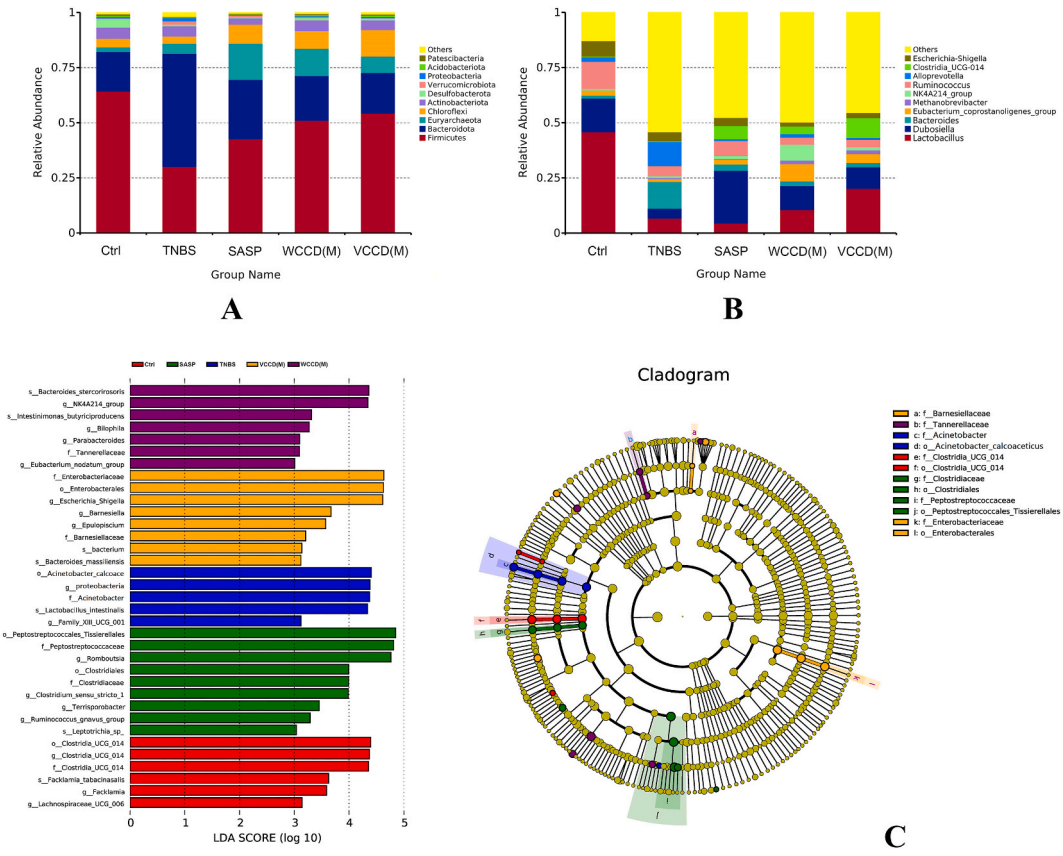

Fig. 5. (A) Microbial community bar plot at the phylum level. (B) Microbial community bar plot at the genus level. (C) LEfSe statistical results.

treatment of ulcerative colitis.

According to the relative expression levels between the two samples, DEGs can be divided into upregulated genes and downregulated genes. Upregulated genes were expressed at higher levels in the drug administration group than those in the control group; conversely, they were downregulated. Fold change (FC) ≥ 1.5 and false discovery rate (FDR) < 0.05 were used as the screening criteria during the DEG assay. FC indicates the ratio of expression between two samples. The FDR was obtained by correcting the p-value for the significance of the difference. Analysis of the DEG clusters in the heat map revealed clustering of DEGs, indicating good reproducibility of the treatments (Fig. 6A). The volcano plot allows a quick look at the differences in gene expression levels between the two samples and the statistical significance of the differences. In the comparison between VCCD(M) and TNBS groups, 1441 DEGs were found, of which 1293 genes were upregulated, and 148 were downregulated (Fig. 6B and C).

3.10. Go and KEGG enrichment analysis

GO enrichment analysis was performed on DEGs in the TNBS and VCCD(M) groups. The top 20 functionally enriched categories were screened for analysis, of which biological process (BP), cellular component (CC), and molecular function (MF) results were shown in Fig. 7. The DEG in BP was mainly concerned with ER to Golgi vesicle-mediated transport, intracellular protein transport, retrograde vesicle-mediated transport, Golgi to ER, cell cycle (Fig. 7A); The DEG in CC was mainly concerned with mitochondrion, proteasome accessory complex and ribonucleoprotein complex (Fig. 7B); The DEG in MF was mainly concerned with mRNA binding, protein domain specific binding, ATPase activity, polyubiquitin binding, GDP binding etc. (Fig. 7C).

A total of 32 pathways were significantly enriched by comparing the VCCD(M) and model groups. Fig. 7D and E shows the bubble and bar graphs of the 20 pathways with the most significant differences in the enrichment analysis of DEGs. Among the pathways between the VCCD(M) and model groups, Erbb Signaling Pathway (ERBB) was the most significant and exceptionally noticeable (Fig. 7F). Transcriptomics showed that in the ERBB pathway, gene expression of NCK2, PAK4 and JNK was down-regulated in the VCCD(M) group compared with the model group, and the results are shown in Table 6. Therefore, we hypothesized that VCCD(M) may inhibit the angiogenic pathway in ERBB by down-regulating the expression of NCK2, PAK4 and JNK, which in turn inhibits inflammation and reduces the risk of developing ulcerative colitis.

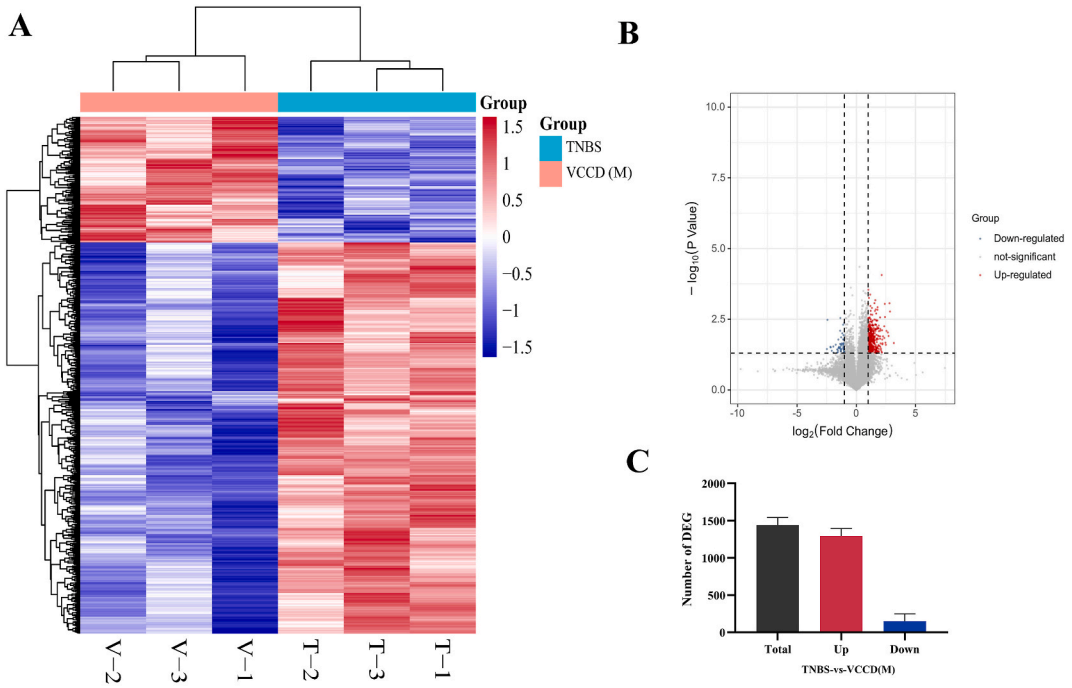

Fig. 6. Analysis of DEGs between VCCD(M) vs TNBS. (A) Heat map of expression patterns of all DEGs. (B) Volcano plot of expression patterns of all DEGs. (C) Histogram showing the number of DEGs; the values are presented as means ± SD (n = 3).

3.11. Western blot

To further confirm the ability of VCCD(M) to ameliorate colonic inflammation in rats, the angiogenic pathway-related proteins NCK2, PAK4, and JNK in the Erbb pathway were selected for validation. The results confirmed that VCCD(M) downregulated the transcription of NCK2, PAK4, and JNK genes (Fig. 8B). In the pre-DEG data, NCK2, PAK4, and JNK expression were downregulated. Subsequently, Western blot (Fig. 8A) was used to detect the expression of angiogenic pathway-related proteins. The results showed that the expression of NCK2, PAK4, JNK, and p-JNK was significantly elevated in colon tissues of the TNBS group compared with the Ctrl group ($P < 0.05$) (Fig. 8C); NCK2, PAK4, JNK, and p-JNK expression was significantly reduced in the VCCD group compared with the TNBS group ($P < 0.05$) (Fig. 8C).

4. Discussion

In this study, two types of cornu cervi degelatinatum were prepared using vinegar-processing and water-processing methods, respectively (Fig. 9). During the Liu Song era, Lei Xiao summarized the accounts and experiences of his predecessors in processing and wrote *Lei Gong Pao Zhi Lun*, the first processing monograph in China [16]. *Lei Gong Pao Zhi Lun* recorded the processing method of cornu cervi degelatinatum is to saw the antlers into segments and place them in running water for 100 days, wash them, added vinegar decoction for seven days and then collect the filter residue and dry it [9]. We optimized the vinegar-processing method of cornu cervi degelatinatum in *Lei Gong Pao Zhi Lun* by using modern high-temperature and high-pressure technology, shortened the processing time, and prepared VCCD (Fig. 9B). Meanwhile, we prepared WCCD (Fig. 9A) by replacing vinegar with water based on the processing method of *Chinese Pharmacopoeia (2020)* [7]. Then, we explored the differences in chemical composition and pharmacological effects of the two cornu cervi degelatinatum using relevant experimental methods such as 16S rRNA, animal experiments, and transcriptomics.

As a common inflammatory bowel disease, UC is characterized by chronic inflammation and ulceration, with the characteristics of continuity and diffuseness, and the disease has a recurrent course, which makes it a common digestive system complication [17]. Spleen and kidney yang deficiency is the basis of recurrent and prolonged UC, therefore, patients with spleen and kidney yang deficiency evidence of UC can be considered to warm the spleen and kidney to enhance the body's immunity, so as to achieve the purpose of treatment of UC. After reviewing the relevant literature and adopting the idea of "combining disease and evidence", we first established spleen and kidney yang deficiency and then constructed the UC rat model [18]. Apply modern pharmacology animal modeling method, make modern medicine disease Chinese medicine evidence model. Therefore, the replication of spleen and kidney yang deficiency type UC rat model can realize the organic combination of "disease" and "evidence", which is more targeted and scientific, and is conducive to the further elaboration of the overall concept of Chinese medicine and the idea of evidence-based treatment. It is conducive to the further interpretation of the holistic concept of Chinese medicine and the idea of recognizing and

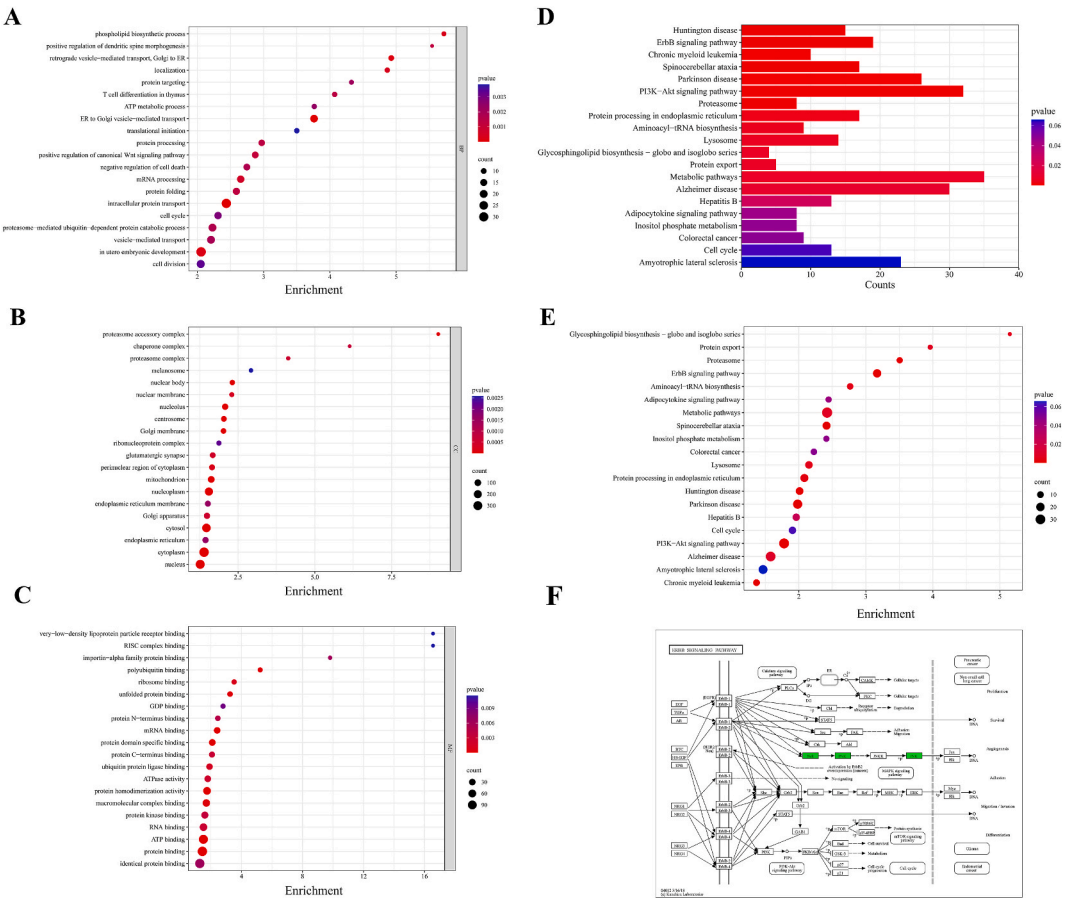

Fig. 7. GO and KEGG enrichment analysis of DEGs in VCCD(M) vs TNBS. (A) Each GO term under BP is enriched. (B) Each GO term under CC is enriched. (C) Each GO term under MF is enriched. (D) Histogram of the enrichment of DEGs in the KEGG pathway. (E) Bubble diagram of KEGG pathway enrichment for DEGs. (F) Erbb Signaling Pathway.

Table 6
Gene Expression of the Erbb Signaling Pathway in colon (FPKM).

Gene symbol	TNBS-1	TNBS-2	TNBS-3	VCCD(M)-1	VCCD(M)-2	VCCD(M)-3
NCK2	29.54	25.46	29.31	17.67	21.17	21.56
PAK4	36.76	28.55	34.59	19.93	22.83	24.31
JNK	1.18	1.05	1.19	0.64	0.74	0.82

treating the disease.

CCD is one of the representatives of warming the spleen and kidney, *Chinese Pharmacopoeia (2020)* [7] recorded that CCD has the function of warming the kidney and helping the yang, astringent and stopping hemorrhage, which is used for spleen and kidney yang deficiency, sores and ulcers that do not astringent and other symptoms. However, the specific mechanism of action of CCD has not been clarified, therefore, a relevant animal model combining disease and evidence was established to study the mechanism of action of CCD in the treatment of UC. The differences in the pharmacological effects of the two CCDs were compared using a spleen and kidney yang deficiency type ulcerative colitis model. It was found that VCCD decreased the levels of pro-inflammatory factors and elevated the levels of anti-inflammatory factors, which was superior to that of WCCD. Further experiments showed that VCCD could increase the number of beneficial bacterial flora in the intestinal tract of rats and reverse TNBS-induced colonic damage.

Firmicutes and *Bacteroidota* are the two most abundant phyla in the intestinal flora, and the ratio of *Firmicutes/Bacteroidota (F/B)* is usually associated with intestinal inflammation [19]. The WCCD and VCCD groups in this study significantly increased the intestinal microflora species, suggesting that CCD can improve the imbalance of intestinal microflora in rats. Short-chain fatty acids (SCFA) are produced by specific bacteria by catabolizing fibers, which serve as an important energy supply in the maintenance of epithelial cells [20]. The production of SCFAs can alter tight junction protein expression, which may be the mechanism by which *Prevotellaceae* and *Lachnospiraceae* improve UC. Species diversity analysis showed that *Akkermansia* in the VCCD group differed significantly from the

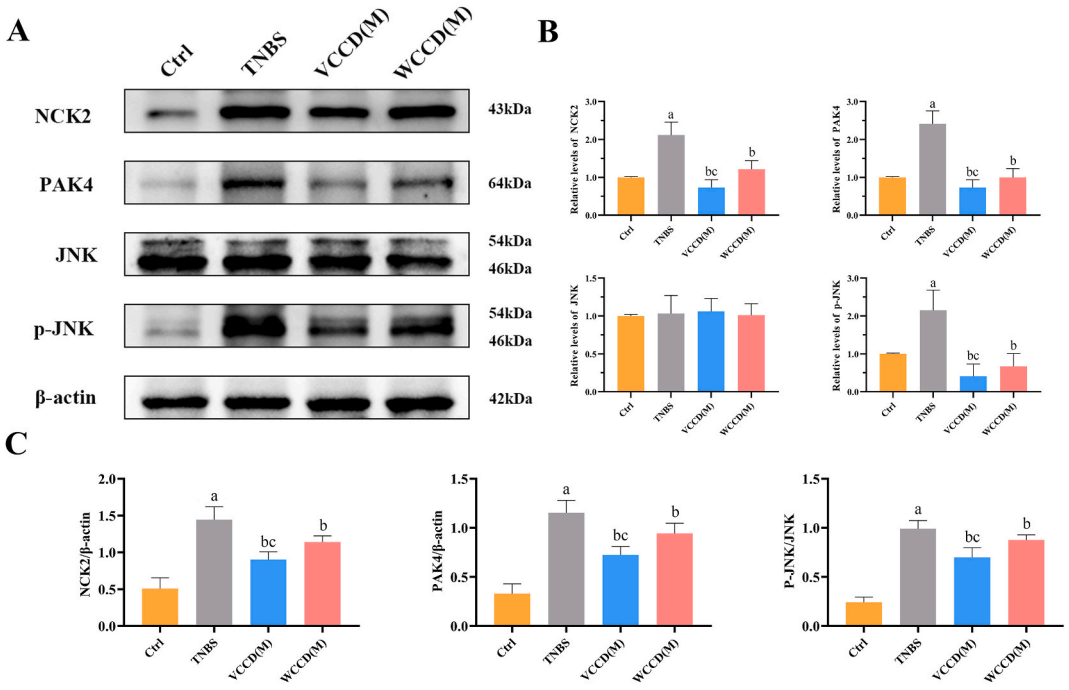

Fig. 8. Western blot images of NCK2, PAK4 and JNK. (A) WB strip map of NCK2, PAK4 and JNK. (B) Related levels of NCK2, PAK4, JNK, p-JNK (mean ± SD, n = 3). (C) Bar plot indicated the statistical analysis of Figure A (means ± SD, n = 3). Different letters indicated statistically significant differences, compared to the control group, $^{a}P < 0.05$; compared to the model group, $^{b}P < 0.05$; compared to the WCCD(M) group, $^{c}P < 0.05$. Complete and unadjusted blot images are shown in Supplementary Data, and blot images of p-JNK are shown in Fig. S1 A-C, JNK are shown in Fig. S2 A-C, PAK4 are shown in Fig. S3 A-C, NCK2 are shown in Fig. S4 A-C, β-actin are shown in Fig. S5 A-C.

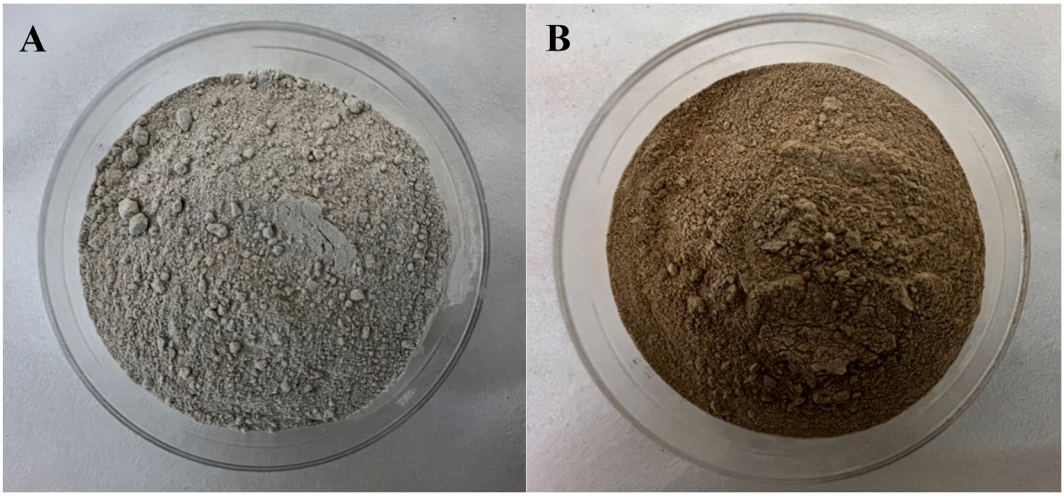

Fig. 9. Water-processed cornu cervi degelatinatum and vinegar-processed cornu cervi degelatinatum. (A) Water-processed cornu cervi degelatinatum. (B) Vinegar-processed cornu cervi degelatinatum.

other administered groups. *Akkermania*, an intestinal mucin degrading bacterium belonging to *Verrucosa*, can produce beneficial SCFAs and vitamins, release anti-inflammatory vesicles, increase mucus thickness, improve intestinal permeability, and reduce inflammatory responses [21].

In the present study, the characteristic flora of the feces of control rats were mostly *Clostridium*, a genus of the family *Bacillaceae*, capable of forming spores and anaerobically growing Gram-staining-positive large bacilli, most of which are non-pathogenic and therefore widely distributed in the normal flora [22]. *Lachnospira* belongs to the *Firmicutes*, which is a potentially beneficial bacterium involved in metabolism of a wide range of carbohydrates and provides energy to the host, and is also distributed in the normal flora

[23]. At the phylum level, the F/B of the model group was higher than that of the control group, which showed similar characteristics to the human UC flora, and the F/B values of all drug groups decreased by drug treatment, with the most obvious decrease in the VCCD group, which favored the production of SCFAs in the intestinal tract [24], and could exert anti-inflammatory effects either directly or indirectly, which indicated that VCCD improved the disorder of the intestinal flora to a certain extent, protected the intestinal barrier function, and regulate metabolism and immunity in rats. The enrichment of *Proteobacteria* was also closely related to the activity degree of UC and markers of inflammation [25]. WCCD and VCCD can restore the abundance of *Proteobacteria* and *Bacteroidetes* at the phylum level, and restore the structure of intestinal flora to a certain extent.

Our sequencing results of gut microorganisms showed significant differences between groups. Pathogenic or conditionally pathogenic bacteria such as *Escherichia_Shigella* in *Proteobacteria* were the dominant species in the feces of rats in the TNBS group. After colonization in vivo, *Escherichiai_Shigella* can invade the intestinal tract by releasing bacterial endotoxin and lead to typical bacillary dysentery, the bacteria in *Proteobacteria* are mostly adherent and invasive, which can induce pro-inflammatory responses and eventually lead to the formation of UC [26]. While the abundance of *Lactobacillus* was significantly higher in the WCCD and VCCD groups than in the TNBS group, as a probiotic, the high abundance of *Lactobacillus* is a good indicator of health. WU Z L et al. [27]. found that the intestinal flora of patients with diarrhea undergoes significant changes, with a decrease in the number of *Lactobacillus* and a decrease in *Clostridium*, *Helicobacter pylori* and other harmful bacteria increased in number, where the trend of *Lactobacillus* is consistent with what we found in our experiment.

In addition, transcriptomics and related experimental studies have shown that VCCD inhibits the ERBB process and suppresses inflammation by delaying angiogenesis through down-regulation of the expression of NCK2, PAK4, and JNK genes and proteins in colonic tissues.

The Erbb signaling pathway is a tyrosine kinase receptor that spans the cell membrane. When different ligands bind to the receptor in normal cells, ERBB family members produce homo or heterodimers, undergo autophosphorylation, and activate different phosphorylation sites to provide docking targets for downstream molecules [28]. EGF and NRG4 ligands activate signaling pathways such as PI3K-Akt, MAPK/ERK, Jak-STAT, and Src-FAK. The MAPK/ERK pathway has four main branches: ERK, JNK, p38/MAPK, and ERK5, of which JNK and p38 are functionally similar and are associated with inflammation, apoptosis, and growth [29]. Stress-activated protein kinase (c-Jun amino-terminal kinase), also known as JNK, is a member of the MAPK family and can be activated by different environmental stresses, inflammatory cytokines, growth factors, and GPCR agonists. Thus JNK plays an important role in metabolism and inflammation [30].

In the process of angiogenesis, endothelial cells play a crucial role. VEGF belongs to the vascular endothelial growth factor family, which promotes the increase of vascular permeability, migration, proliferation of vascular endothelial cells and angiogenesis [31]. MAPK signaling pathway is an important pathway for the occurrence of cellular responses, and it has an important role in the regulation of cell proliferation, differentiation, and apoptosis. JNK, as a member of MAPK family , and in the JNK pathway, p-JNK is activated to initiate downstream signaling events, leading to the release of inflammatory factors and an increase in general inflammation [32]. Therefore, it has been found that the process of angiogenesis can be inhibited by inhibiting JNK activation, which leads to a reduction in colonic injury and a decrease in non-specific inflammatory responses [33].

Increased vascular permeability is an important component of inflammation, which leads to tissue damage and organ failure. Previous studies have shown that p21-activated kinase (PAK), a key regulator of cell junctions, regulates endothelial cells by affecting myosin light chain phosphorylation and cell contractility [34]. It is now shown that blocking PAK function inhibits inflammation, and in endothelial cells, myosin light chain phosphorylation induced by PAK is mediated by mitogen-activated protein kinases and extracellular signal-regulated kinases (Erk). Erk in the lungs of lipopolysaccharide (LPS)-treated mice is dependent on PAK activation in cells, most prominently the vascular endothelium. Activation of Erk requires the integrity of the complex between PAK, PIX, and GIT1, and lung injury in mice can be inhibited by blocking PAK binding to PIX [35]. This PAK complex can be found to be essential for Erk-dependent myosin phosphorylation and vascular permeability. It can be concluded that by inhibiting the PAK signaling pathway, vascular permeability can be inhibited, thereby reducing nonspecific inflammation.

NCK2 is a binding protein, NCK2 binds to receptor tyrosine kinases and phosphorylates tyrosine residues via SH2; it binds to recruit actin regulatory proteins such as WASP, Dock180 and PAK via SH3, and further regulates actin aggregation and alignment via nucleating proteins such as Arp2/3 and MLC [36]. NCK2 has also been reported to be extensively involved in coordinating various signaling pathways, including those of growth factor receptors and cell adhesion receptors. However, NCK2 has been rarely reported as an upstream regulatory protein of PAK4 in the JNK/p38 and MAPK signaling pathways.

In conclusion, vinegar processing increased the content of Gly, Glu, and Asp, as well as minerals in cornu cervi degelatinatum. VCCD decreased DAI and CMDI scores, maintained homeostasis of inflammatory factors in the body, and promoted the increase of beneficial intestinal bacteria. It reversed TNBS-induced colonic damage, and its effect was superior to that of WCCD. In addition, transcriptomics and related experiments showed that VCCD reduced the expression of NCK2, PAK4 and JNK genes and proteins in rat colon, and inhibited the process of ERBB by delaying angiogenesis, which resulted in the therapeutic effect on ulcerative colitis.

Funding

This research was funded by Major Science and Technology Projects in Jilin Province (No. 20220304001YY).

Ethics statement

All experiments were performed under the guidelines for animal experiments at Jilin Agricultural University. The agreement was

approved by the Institutional Animal Ethics and Use Committee of Jilin Agricultural University (Permit number: 20211011003). Laboratory animal use license of laboratory animal center of Jilin Agricultural University: SYXK (Ji) 2018-0023. Approval date: October 11, 2021.

Data availability statement

Data related to this study were not deposited in publicly available repositories. Data related to this study will be provided upon request.

CRediT authorship contribution statement

Tianshi Li: Writing – review & editing, Writing – original draft, Methodology, Conceptualization. **Mengqi Shi:** Writing – review & editing, Writing – original draft, Methodology, Conceptualization. **Yan Zhao:** Writing – review & editing, Writing – original draft, Methodology, Conceptualization. **Zhongmei He:** Software. **Ying Zong:** Software. **Weijia Chen:** Data curation. **Rui Du:** Data curation.

Declaration of competing interest

The authors declare that they have no known competing financial interests or personal relationships that could have appeared to influence the work reported in this paper.

Acknowledgements

The authors thank Yan Zhao for critically reviewing the manuscript and English editing.

Appendix A. Supplementary data

Supplementary data to this article can be found online at https://doi.org/10.1016/j.heliyon.2024.e24782.

References

[1] W. Cheng, X. Wang, Y. Wu, et al., Huanglian-Houpo extract attenuates DSS-induced UC mice by protecting intestinal mucosal barrier and regulating macrophage polarization [J], J. Ethnopharmacol. (2023) 307, https://doi.org/10.1016/j.jep.2023.116181.
[2] P. Wang, J. Hu, S. Ghadermarzi, et al., Smoking and inflammatory bowel disease: a comparison of China, India, and the USA [J], Dig. Dis. Sci. 63 (10) (2018) 2703–2713, https://doi.org/10.1007/s10620-018-5142-0.
[3] D.E. O'sullivan, R.L. Sutherland, S. Town, et al., Risk factors for early-Onset colorectal cancer: a Systematic review and Meta-analysis [J], Clin. Gastroenterol. Hepatol. 20 (6) (2022) 1229, https://doi.org/10.1016/j.cgh.2021.01.037, 40.e5.
[4] T. Kobayashi, B. Siegmund, C. Le Berre, et al., Ulcerative colitis [J], Nat. Rev. Dis. Prim. 6 (1) (2020) 74, https://doi.org/10.1038/s41572-020-0205-x.
[5] X. Xiucui, Z. Yi, D. Xiahuan, et al., Theoretical discussion and clinical experience of spleen-strengthening and kidney-warming method in treating spleen-kidney-yang-deficiency type ulcerative colitis [J], Sichuan Traditional Chinese Medicine 32 (8) (2014) 24–26.
[6] W. Guishuang, Observation on the curative effect of traditional Chinese medicine in the treatment of ulcerative colitis [J], Modern Journal of Integrated Traditional Chinese and Western Medicine 23 (13) (2014) 1434–1436.
[7] S.P. Committee, Pharmacopoeia of the People's Republic of China: [S], The Medicine Science and Technology Press of China, Beijing, 2020.
[8] Z. Qian, X. Rong, X. Ruijie, et al., Processing theory of "leading vinegar-processing Chinese medicine into liver. [J], Zhongguo Zhong yao za zhi , China journal of Chinese materia medica 47 (18) (2022) 4854–4862, https://doi.org/10.19540/j.cnki.cjcmm.20220307.301.
[9] Z. Jinhuang, A brief introduction of Lei Gong's theory of fire and fire and Lei "s biography [J], Shanghai J. Tradit. Chin. Med. (1) (1957) 33–34, https://doi.org/10.16305/j.1007-1334.1957.01.014.
[10] K. Reinmuth-Selzle, T. Tchipilov, A.T. Backes, et al., Determination of the protein content of complex samples by aromatic amino acid analysis, liquid chromatography-UV absorbance, and colorimetry [J], Anal. Bioanal. Chem. 414 (15) (2022) 4457–4470, https://doi.org/10.1007/s00216-022-03910-1.
[11] L. Qian, L. Feng, W. Wan, et al., Analysis of inorganic elements in deer bone, antlers and pith [J], Chinese Archives of Traditional Chinese Medicine 36 (9) (2018) 2220–2222, https://doi.org/10.13193/j.issn.1673-7717.2018.09.043.
[12] L. Yao, Mechanism of Fuzi Lizhong Decoction on Treg Cell Related Factors in Rats with Ulcerative Colitis of Spleen Kidney Yang Deficiency Type [D], 2021.
[13] A. Heida, M. Knol, A.M. Kobold, et al., Agreement between home-based measurement of stool calprotectin and ELISA results for monitoring inflammatory bowel disease activity [J], Clin. Gastroenterol. Hepatol. 15 (11) (2017) 1742–1749, https://doi.org/10.1016/j.cgh.2017.06.007.
[14] J.G. Caporaso, C.L. Lauber, W.A. Walters, et al., Global patterns of 16S rRNA diversity at a depth of millions of sequences per sample [J], Proc Natl Acad Sci U S A 108 (Suppl 1) (2011) 4516–4522, https://doi.org/10.1073/pnas.1000080107. Suppl 1.
[15] K. Mokhtari, M. Peymani, M. Rashidi, et al., Colon cancer transcriptome [J], Prog. Biophys. Mol. Biol. 180–181 (2023) 49–82, https://doi.org/10.1016/j.pbiomolbio.2023.04.002.
[16] G. Qianfeng, Science of Chinese Medicinal Herbs Preparation: [S], China Press of Traditional Chinese Medicine, Beijing, 2003.
[17] S.S. Seyedian, F. Nokhostin, M.D. Malamir, A review of the diagnosis, prevention, and treatment methods of inflammatory bowel disease [J], Journal of medicine and life 12 (2) (2019) 113–122, https://doi.org/10.25122/jml-2018-0075.
[18] Wangdi Study, On the Effect of Warming Kidney and Strengthening Spleen Method on the Gene Expression of TLR/IL-1 Signaling Pathway Regulators in Colon Tissue of Rats with Ulcerative Colitis [D], 2016.
[19] H. Sokol, P. Seksik, J.P. Furet, et al., Low counts of Faecalibacterium prausnitzii in colitis microbiota [J], Inflamm. Bowel Dis. 15 (8) (2009) 1183–1189, https://doi.org/10.1002/ibd.20903.
[20] H. Si, Q. Yang, H. Hu, et al., Colorectal cancer occurrence and treatment based on changes in intestinal flora [J], Semin. Cancer Biol. 70 (2021) 3–10, https://doi.org/10.1016/j.semcancer.2020.05.004.

[21] F. Wu, X. Guo, M. Zhang, et al., An Akkermansia muciniphila subtype alleviates high-fat diet-induced metabolic disorders and inhibits the neurodegenerative process in mice [J], Anaerobe 61 (2020) 102138, https://doi.org/10.1016/j.anaerobe.2019.102138.
[22] J. Liang, S. Kou, C. Chen, et al., Effects of Clostridium butyricum on growth performance, metabonomics and intestinal microbial differences of weaned piglets [J], BMC Microbiol. 21 (1) (2021) 85, https://doi.org/10.1186/s12866-021-02143-z.
[23] X. Yuan, B. Chen, Z. Duan, et al., Depression and anxiety in patients with active ulcerative colitis: crosstalk of gut microbiota, metabolomics and proteomics [J], Gut Microb. 13 (1) (2021) 1987779, https://doi.org/10.1080/19490976.2021.1987779.
[24] J. Du, M. Yang, Z. Zhang, et al., The modulation of gut microbiota by herbal medicine to alleviate diabetic kidney disease - a review [J], Front. Pharmacol. 13 (2022) 1032208, https://doi.org/10.3389/fphar.2022.1032208.
[25] M.K. Vester-Andersen, H.C. Mirsepasi-Lauridsen, M.V. Prosberg, et al., Increased abundance of proteobacteria in aggressive Crohn's disease seven years after diagnosis [J], Sci. Rep. 9 (1) (2019) 13473, https://doi.org/10.1038/s41598-019-49833-3.
[26] J. Xu, N. Chen, Z. Wu, et al., 5-Aminosalicylic acid alters the gut bacterial microbiota in patients with ulcerative colitis [J], Front. Microbiol. 9 (2018) 1274, https://doi.org/10.3389/fmicb.2018.01274.
[27] Z.L. Wu, R. Wei, X. Tan, et al., Characterization of gut microbiota dysbiosis of diarrheic adult yaks through 16S rRNA gene sequences [J], Front. Vet. Sci. 9 (2022) 946906, https://doi.org/10.3389/fvets.2022.946906.
[28] C.L. Arteaga, J.A. Engelman, ERBB receptors: from oncogene discovery to basic science to mechanism-based cancer therapeutics [J], Cancer Cell 25 (3) (2014) 282–303, https://doi.org/10.1016/j.ccr.2014.02.025.
[29] E.F. Wagner, A.R. Nebreda, Signal integration by JNK and p38 MAPK pathways in cancer development [J], Nat. Rev. Cancer 9 (8) (2009) 537–549, https://doi.org/10.1038/nrc2694.
[30] W. Gao, C. Wang, L. Yu, et al., Chlorogenic acid attenuates Dextran sodium sulfate-induced ulcerative colitis in mice through MAPK/ERK/JNK pathway [J], BioMed Res. Int. 2019 (2019) 6769789, https://doi.org/10.1155/2019/6769789.
[31] Y. Itatani, K. Kawada, T. Yamamoto, et al., Resistance to anti-angiogenic Therapy in cancer-alterations to anti-VEGF pathway [J], Int. J. Mol. Sci. 19 (4) (2018), https://doi.org/10.3390/ijms19041232.
[32] S. Yang, F. Li, S. Lu, et al., Ginseng root extract attenuates inflammation by inhibiting the MAPK/NF-κB signaling pathway and activating autophagy and p62-Nrf2-Keap1 signaling in vitro and in vivo [J], J. Ethnopharmacol. 283 (2022) 114739, https://doi.org/10.1016/j.jep.2021.114739.
[33] B. Yin, H. Tian-Chu, X. Ling-Fen, Protection by microRNA-7a-5p antagomir against intestinal mucosal injury related to the JNK pathway in TNBS-induced experimental colitis [J], Turk. J. Gastroenterol. : the official journal of Turkish Society of Gastroenterology 32 (5) (2021) 431–436, https://doi.org/10.5152/tjg.2021.20746.
[34] M. Wang, C. Zhang, Q. Zheng, et al., RhoJ facilitates angiogenesis in glioblastoma via JNK/VEGFR2 mediated activation of PAK and ERK signaling pathways [J], Int. J. Biol. Sci. 18 (3) (2022) 942–955, https://doi.org/10.7150/ijbs.65653.
[35] R. Stockton, J. Reutershan, D. Scott, et al., Induction of vascular permeability: beta PIX and GIT1 scaffold the activation of extracellular signal-regulated kinase by PAK [J], Mol. Biol. Cell 18 (6) (2007) 2346–2355, https://doi.org/10.1091/mbc.e06-07-0584.
[36] K. Jacquet, S.L. Banerjee, F.J.M. Chartier, et al., Proteomic analysis of NCK1/2 adaptors uncovers paralog-specific interactions that reveal a New role for NCK2 in cell abscission during cytokinesis [J], Molecular & cellular proteomics : MCP 17 (10) (2018) 1979–1990, https://doi.org/10.1074/mcp.RA118.000689.